Multidimensional measures of electromagnetic chirality and their conformal invariance

Maxim Vavilin, Ivan Fernandez-Corbaton

KARLSRUHE INSTITUTE OF TECHNOLOGY

CRC 1173

Participating universities

Universität Stuttgart

EBERHARD KARLS
UNIVERSITÄT
TÜBINGEN

TU
WIEN

Funded by

DFG

Multidimensional measures of electromagnetic chirality and their conformal invariance

Maxim Vavilin[1] and Ivan Fernandez-Corbaton[2]

[1]Institute of Theoretical Solid State Physics, Karlsruhe Institute of Technology, Karlsruhe, Germany
[2]Institute of Nanotechnology, Karlsruhe Institute of Technology, Karlsruhe, Germany

November 3, 2021

Abstract

Proper assignment of left- and right-handed labels to general chiral objects is known to be a theoretically unfeasible problem. Attempts to utilize a pseudoscalar function to distinguish enantiomers face two unavoidable difficulties: false chiral zeros and unhanded chiral states. In here, we demonstrate how both of these problems can be solved in the context of light-matter interactions. First, we introduce a two-dimensional quantity called complex electromagnetic chirality that solves the problem of false chiral zeros. Next, we define an infinite-dimensional pseudovector called chirality signature that completely quantifies the multidimentional nature of electromagnetic chirality, does not have false global chiral zeros, and allows to continuously distinguish any pair of enantiomers. We prove that the introduced measures are invariant under the largest group of symmetries of Maxwell's equations – the conformal group. The complete and conformally invariant quantification of electromagnetic chirality provided by the chirality signature distinguishes it as a particularly suitable tool for the study of chirality and its applications.

1 Introduction

There are two types of objects: those that can be superimposed onto their own mirror image and those that can not. The latter are called chiral objects and they exist in pairs (called enantiomers): an object and its mirror antipode. One often distinguishes between both versions by assigning a label "left" or "right" using a reference or a conventional rule. There are hence two different albeit related concepts: chirality, which is a property of an object to differ from its mirror image, and handedness, which is a label that tells two enantiomers apart.

The concept of chirality underlies a wide spectrum of physical phenomena, ranging from the left-right asymmetry of the weak interaction in particle physics, through the differential response of chiral molecules to different polarization handedness of light, to chiral magnetic fields of galactic scale. Practical aspects

1

of selecting a particular molecular enantiomer are crucial in pharmacy, when both left and right-handed versions of the same chiral molecule are produced in a chemical reaction, but only one has the required medical effect.

It is remarkable that, despite their broad use, the left and right-handed labels can not be appropriately assigned to all chiral objects [1]. A chiral object that is complex enough can be transformed into its mirror image by a continuous transformation such that it stays chiral at all times [2,3], which is known as the chiral connectedness property. Given any classification that assigns left- and right-handed labels, there would be a point of this transformation when the handedness of the object would switch discontinuously. In other words, chiral objects would exist that are arbitrarily similar to each other, but have opposite handedness. In practice such states would be of ambiguous handedness, which would imply the incompleteness of classification: some chiral object could not be distinguished from their enantiomers.

Similarly, attempts to quantify chirality with a continuous real pseudoscalar function face unsolvable difficulties. Under the requirement that such function obtains the value of zero for achiral states and takes values of opposite signs for enantiomeric configurations, the chiral connectedness implies that the function would also have to acquire a value of zero at some chiral point [1]. In this case one speaks of a false chiral zero – the zero value of the pseudoscalar function can not definitively indicate an achiral state. However, as we will show, if one additionally augments the pseudoscalar function with an indicator that could tell apart chiral objects from achiral ones, then all objects can be cast into four sets: achiral, left-handed, right-handed and unhanded (chiral states with zero value of pseudoscalar function). If an object belongs to the latter class, it can not be distinguished from its mirror antipode in this description. However, the set of such objects happens to be vanishingly small compared to the handed sets, which suggests that this classification may be useful in some practical applications.

Weinberg and Mislow argued in [1] that problems of assigning handedness labels reflect the multidimensional nature of chirality. They showed that utilization of one or several pseudoscalar properties of an object, such as optical rotation and circular dichroism, is, in general, not sufficient to describe its chirality completely. It was conjectured that an infinite-dimensional pseudovector should exist that consists of pseudoscalar components, each acting as an independent handedness measure. Although each of the components would individually have false chiral zeros, the achiral configuration could still be identified by the condition that all components vanish simultaneously. The norm of such vector would define an appropriate scalar measure of chirality. Scalar measures of chirality, also known as degrees of chirality, quantify how much an object differs from its mirror antipode without distinguishing one enantiomer from the other. Defining such quantities has its own challenges, such as non-uniqueness [4] and the lack of upper bound. The rich history of attempts to quantitavely describe chirality and the discussion of corresponding difficulties is reviewed in [4].

In this paper, we study the chirality of objects by reference to their interaction with the electromagnetic field. We do not focus on individual chiral properties such as optical rotation or circular dicroism, but instead we use the T-matrix method [5, 6]. The T-matrix (or transition operator) contains the complete information about the linear interaction of an object with dynamic electromagnetic fields, allowing to formalize chirality measures as functions on

the spaces of T-matrices. Additionally, there is an abundance of resources that numerically compute T-matrices of various systems [7], including the calculation of T-matrices for molecules from quantum-mechanical simulation data [8].

Previously [9] the use of the T-matrix method allowed to reinterpret chirality in the context of electromagnetic scattering by measuring how differently the object interacts with fields of opposite polarization handedness. The new property was called electromagnetic chirality (em-chirality), and its scalar measure was introduced as well. This measure has an upper bound with the remarkable characteristic that maximally em-chiral reciprocal objects are invisible to all light of a particular polarization handedness. Efforts to design and fabricate materials with such properties are ongoing [10–12]. The notion of em-chirality is also being considered in applied mathematics [13, 14], and its mechanical counterpart can play a role in mechanical metamaterials [15].

In the present article we will extend the discussion of em-chirality by solving two problems. The first one is the quantification of handedness without false chiral zeros. For this we consider one particular pseudoscalar property of a scatterer and combine it with the scalar measure of em-chirality. We render the result as a complex-valued function called complex em-chirality. It features the scalar em-chirality as its absolute value and the pseudoscalar function as its real part. Zero values of the pseudoscalar property will only contribute to the zero value of the real part of the complex number – the question whether an object is chiral or achiral is then addressed by the absolute value, which allows to separate achiral states from unhanded states.

The second problem that we solve is the complete description of em-chirality that allows to continuously distinguish any two enantiomers. We introduce an infinite-dimensional pseudovector called chirality signature, whose pseudoscalar components vanish simultaneously if and only if the configuration is em-achiral. This provides, for the first time, the complete quantification of the multidimensional nature of chirality that Weinberg and Mislow envisioned in [1]. Despite its infinite-dimentionality it can be practically calculated and represented, because it admits an appropriate truncation.

Importantly, we show that the chirality signature, and the scalar and complex measures of em-chirality are invariant under the group of conformal transformations, which is the largest group of symmetries of Maxwell's equations. This means, in particular, that each chirality signature is uniquely associated with a corresponding set of objects, where all objects in the set are related to each other by conformal transformations.

Additionally, we provide numerical computations of the introduced measures for selected configurations of dielectric spheres and their continuous rearrangements in monochromatic regime. We use complex em-chirality to illustrate the chiral connectedness property and to solve the false chiral zeros problem. We also represent the chirality signature of chiral and achiral configurations, capturing the em-chirality of the considered system in its multidimensional entirety.

The article is organized as follows. Sections 2 and 3 provide the context for the core Sections 4 to 7. Section 2 contains an overview of the helicity operator and the T-matrix method, which are two central concepts for the study of electromagnetic chirality. Section 3 contains a brief exposition of the em-chirality and its scalar measure that were previously introduced in [9], including a new equivalent alternative definition of em-chirality as the solution of a Procrustes-like minimization problem. In Sec. 4 we define the complex em-chirality and

then use it in Sec. 5 to illustrate a solution to the false chiral zeros problem. Section 6 is devoted to the chirality signature. In Sec. 7 we prove the conformal invariance of the introduced measures, and Sec. 8 contains the final remarks.

2 Helicity and the T-matrix

2.1 Electromagnetic helicity as chirality reference

When studying chirality of any object one is often interested in a reference that changes its property under mirror transformations. In the context of light-matter interactions the role of such reference is played by the polarization handedness of light, or, more fundamentally, the electromagnetic helicity. The role of helicity in chiral light-matter interactions is under intense scrutiny [16–29]. We can split any electromagnetic field into two components of opposite helicity, left-handed and right-handed, corresponding to eigenstates of the helicity operator Λ with eigenvalue $\lambda = 1$ and $\lambda = -1$, respectively. The helicity operator Λ is defined as the projection of the angular momentum operator onto the direction of the linear momentum operator

$$\Lambda = \frac{\boldsymbol{J} \cdot \boldsymbol{P}}{|\boldsymbol{P}|}. \tag{1}$$

The fundamental importance of helicity arises from the invariance of the helicity operator Λ under translations, rotations and Lorentz boosts [30, Sec. 10.4]. This fact is embedded in the theory of special relativity: since the speed of light is maximal, it is impossible to boost a reference frame such that the photon would reverse its direction, which means that the projection of its angular momentum onto its direction can not switch under changes of reference frames. The parity transformation, however, anticommutes with the helicity operator Λ and hence changes the sign of λ, which makes helicity a natural chirality reference in light-matter interactions. In this article we will be using the helicity basis for representing states of the electromagnetic field, and the operators describing the light-matter interactions.

In the space of solutions of Fourier-transformed Maxwell's equations in an empty source-free region the helicity operator in Eq. (1) is represented by the curl operator divided by the wavenumber

$$\Lambda \to \frac{1}{k} \boldsymbol{\nabla} \times . \tag{2}$$

2.2 The T-matrix method

One of the most powerful and efficient methods of theoretical study of various scattering problems is the T-matrix method. Usually one considers a monochromatic electromagnetic field in the presence of a scatterer that is enclosed in a sphere of radius R around the origin. The Fourier-transformed Maxwell's equations for the empty source-free region outside of this sphere read

$$\boldsymbol{\nabla} \times \boldsymbol{E} = ikZ_0\boldsymbol{H}, \qquad\qquad \boldsymbol{\nabla} \times \boldsymbol{H} = -ik\boldsymbol{E}/Z_0 \tag{3}$$

$$\boldsymbol{\nabla} \cdot \boldsymbol{E} = 0, \qquad\qquad \boldsymbol{\nabla} \cdot \boldsymbol{H} = 0, \tag{4}$$

4

where $Z_0 = \mu_0 c$ is the impedance of the free space, $k = |\boldsymbol{k}| = \omega/c > 0$ is the length of the wave vector, and the harmonic time-dependence $e^{-i\omega t}$ is omitted. The general solution can be decomposed in electric $\boldsymbol{N}_{jm}$ and magnetic $\boldsymbol{M}_{jm}$ multipoles [6]:

$$\boldsymbol{E}_{tot}(\boldsymbol{r}) = \sum_{j=1}^{\infty} \sum_{m=-j}^{j} a_{jm} \operatorname{Rg} \boldsymbol{M}_{jm}(\boldsymbol{r}) + b_{jm} \operatorname{Rg} \boldsymbol{N}_{jm}(\boldsymbol{r}) \tag{5}$$

$$+ \sum_{j=1}^{\infty} \sum_{m=-j}^{j} c_{jm} \boldsymbol{M}_{jm}(\boldsymbol{r}) + d_{jm} \boldsymbol{N}_{jm}(\boldsymbol{r}), \quad |\boldsymbol{r}| > R, \tag{6}$$

with

$$\operatorname{Rg} \boldsymbol{M}_{jm}(\boldsymbol{r}) = j_j(kr)(-i)\boldsymbol{r} \times \boldsymbol{\nabla} \frac{Y_{jm}(\theta, \phi)}{\sqrt{j(j+1)}} \tag{7}$$

$$\operatorname{Rg} \boldsymbol{N}_{jm}(\boldsymbol{r}) = \frac{1}{k} \boldsymbol{\nabla} \times \operatorname{Rg} \boldsymbol{M}_{jm}(\boldsymbol{r}) \tag{8}$$

and

$$\operatorname{Rg} \boldsymbol{M}_{jm}(\boldsymbol{r}) = \frac{1}{k} \boldsymbol{\nabla} \times \operatorname{Rg} \boldsymbol{N}_{jm}(\boldsymbol{r}), \tag{9}$$

where a_{jm} and b_{jm} are expansion coefficients, $j_j(\cdot)$ are spherical Bessel functions and $Y_{jm}(\theta, \phi)$ are the spherical functions as defined in [31, Sec. 3.5].

The magnetic field is simply given by

$$\boldsymbol{H}_{tot}(\boldsymbol{r}) = \frac{i}{k} \boldsymbol{\nabla} \times \boldsymbol{E}_{tot}(\boldsymbol{r}). \tag{10}$$

The irregular terms in (6) are acquired by interchanging spherical Bessel functions $j_j(\cdot)$ for spherical Hankel functions of the first kind $h_j^{(1)}(\cdot)$. The regular term (5) is called the incident field $\boldsymbol{E}_i$ and the irregular (6) is called the scattered field $\boldsymbol{E}_s$.

The complete information about linear interaction of an object with dynamic electromagnetic fields is contained in its T-matrix [6]. It connects the coefficients of the incident and the scattered fields:

$$T \begin{pmatrix} \vec{a} \\ \vec{b} \end{pmatrix} = \begin{pmatrix} \vec{c} \\ \vec{d} \end{pmatrix}, \tag{11}$$

where $\vec{a}$, $\vec{b}$, $\vec{c}$, and $\vec{d}$ are composed of the coefficients a_{jm}, b_{jm}, c_{jm}, and d_{jm}, respectively.

While the T-matrix is most often considered for monochromatic fields, group-theoretical arguments allow the generalization to poly-chromatic fields. Such generalization will be the subject of a dedicated article. We now describe here the few aspects that are necessary for the present article.

First, we change the multipole basis to a multipole basis of eigenstates of the helicity operator:

$$\operatorname{Rg} \boldsymbol{A}_{\lambda jm}(\boldsymbol{r}, \omega) := \frac{1}{\sqrt{2}} \Big(\operatorname{Rg} \boldsymbol{M}_{jm}(\boldsymbol{r}, \omega) + \lambda \operatorname{Rg} \boldsymbol{N}_{jm}(\boldsymbol{r}, \omega) \Big) \tag{12}$$

for helicity $\lambda = \pm 1$. The property

$$\frac{\boldsymbol{\nabla}}{k} \times \text{Rg}\,\boldsymbol{A}_{\lambda j m}(\boldsymbol{r}, \omega) = \lambda \,\text{Rg}\,\boldsymbol{A}_{\lambda j m}(\boldsymbol{r}, \omega) \tag{13}$$

follows from (8) and (9).

Next, we use the results of [32, Eqs. (33b)-(33c)] to write the incident polychromatic field as

$$\boldsymbol{E}_i(\boldsymbol{r}, t) = \sum_{\lambda = \pm 1} \sum_{j=1}^{\infty} \sum_{m=-j}^{j} \int_{>0}^{\infty} d\omega \, \omega(i)^{j-1} f_{jm\lambda}(\omega) \text{Rg}\,\boldsymbol{A}_{\lambda j m}(\boldsymbol{r}, \omega) e^{-i\omega t}. \tag{14}$$

The main advantage of this representation lies in the transformation properties of coefficients $f_{jm\lambda}(\omega) \propto a_{jm} + \lambda b_{jm}$. As discussed in [32], they transform under unitary irreducible representations of the Poincaré group for zero mass and helicity $\lambda = \pm 1$ in the multipolar basis. In particular, each helicity eigenstate transforms independently. That is, the two helicities do not mix upon transformations of the Poincaré group. We will use these transformations properties for proving invariance properties of em-chirality in Sec.7. We also note that the scattered field (6) can be written in the same form as eq.(14) by exchanging $j_j(\cdot)$ for $h_j^{(1)}(\cdot)$. Transformation properties of the scattered field coefficients are the same as of the incident field, since spherical Hankel functions are defined by the same differential equations as the spherical Bessel functions [33]. The T-matrix can now be re-interpreted as an operator that acts in the Hilbert space of irreducible representations of the Poincaré group labeled by zero mass and helicity $\lambda = \pm 1$. A state in this space can be written as [32]:

$$|f\rangle = \sum_{\lambda = \pm 1} \sum_{j=1}^{\infty} \sum_{m=-j}^{j} \int_{>0}^{\infty} \frac{d\omega}{\omega} f_{jm\lambda}(\omega) \, |\omega j m \lambda\rangle \tag{15}$$

$$= \sum_{\lambda = \pm 1} \int \frac{d^3\boldsymbol{p}}{|\boldsymbol{p}|} f_\lambda(\boldsymbol{p}) \, |\boldsymbol{p}\lambda\rangle. \tag{16}$$

Equation (15) is the decomposition in the angular momentum basis states $|\omega j m \lambda\rangle$, which are eigenvectors of four operators $\boldsymbol{P}^2$, J^2, J_3 and Λ, while Eq. (16) is the decomposition in the plane wave basis where $|\boldsymbol{p}\lambda\rangle$ are eigenvectors of P_1, P_2, P_3, and Λ. The state functions are square-integrable with respect to the scalar product

$$\langle f|h \rangle = \sum_{\lambda = \pm 1} \sum_{j=1}^{\infty} \sum_{m=-j}^{j} \int_{>0}^{\infty} \frac{d\omega}{\omega} f_{jm\lambda}^*(\omega) h_{jm\lambda}(\omega), \tag{17}$$

whose equivalent expression in the plane-wave basis is

$$\langle f|h \rangle = \sum_{\lambda = \pm 1} \int \frac{d^3\boldsymbol{p}}{|\boldsymbol{p}|} f_\lambda^*(\boldsymbol{p}) h_\lambda(\boldsymbol{p}). \tag{18}$$

The value of $\langle f|h \rangle$ is invariant under the action of the Poincaré group (corresponds to the unitarity property). In fact, Gross [34] showed that this scalar

6

product is also invariant under the conformal group – the largest group of symmetries of Maxwell's equations. The conformal group extends the Poincaré group with dilations and special conformal transformations. The latter have been connected to physical accelerations [35, 36].

It is straightforward to restrict this generalized T-operator to a single-frequency description, recovering the common monochromatic T-matrix. One benefit of the non-monochromatic description consists in the ability to describe objects that change the frequencies in the scattering process, such as in Raman scattering. Moreover, the general T-operator is necessary for considering Lorentz transformations, dilations, and special conformal transformations, since all these transformations change the frequency content of the electromagnetic field.

3 Electromagnetic chirality

Since the linear interaction of a scatterer with dynamic electromagnetic fields is completely described by its T-operator, it is essential to define chirality as a function on the space of T-operators. In [9], the T-operator approach allowed to introduce the notion of *electromagnetic chirality* (em-chirality) and its scalar measure, which reflects how differently the object interacts with fields of opposite helicity. In this interpretation chirality becomes a Lorentz-invariant property that includes the usual geometric chirality as a special case. The scalar measure of em-chirality admits a maximal value that depends on the total interaction of the object with the electromagnetic field, and indicates invisibility to fields of a particular polarization handedness. In this section we provide a short exposition of the corresponding results.

A T-operator in the helicity basis

$$T = \begin{pmatrix} T^{++} & T^{+-} \\ T^{-+} & T^{--} \end{pmatrix} \tag{19}$$

consists of four suboperators $T^{\lambda\lambda'}$ that act on states with helicity $\lambda' = \pm 1$ and map them to states with helicity $\lambda = \pm 1$. Electromagnetically achiral objects are defined as those that satisfy

$$T^{++} = U_1 T^{--} V_1 \tag{20}$$
$$T^{-+} = U_2 T^{+-} V_2 \tag{21}$$

for some unitary $U_{1,2}$ and $V_{1,2}$. This condition indicates whether measurements done with incident fields of a particular polarization handedness are unitarily similar to the measurements done with incident fields of the opposite polarization handedness [9].

The definition of em-chirality contains the common geometric definition of chirality, because translations and rotations act unitarily on the T-suboperators and do not change the polarization handedness of the EM-field.

But since the set of unitary transformations is larger than the set of rotations and translations, there exist geometrically chiral objects that are not electromagnetically chiral, for example those that fulfill Eqs. (20)-(21) with Lorentz transformations and not with rotations or translations.

To answer the question, to which degree a given scatterer is electromagnetically chiral, the scalar measure of em-chirality χ was introduced in [9] using the

sequences of singular values of the suboperators [1] :

$$\chi(T) = \sqrt{\sum_k \left(\sigma_k(T^{++}) - \sigma_k(T^{--})\right)^2 + \sum_k \left(\sigma_k(T^{+-}) - \sigma_k(T^{-+})\right)^2} \qquad (22)$$

$$=: \sqrt{|\vec{\sigma}(T^{++}) - \vec{\sigma}(T^{--})|^2 + |\vec{\sigma}(T^{+-}) - \vec{\sigma}(T^{-+})|^2}, \qquad (23)$$

where $\vec{\sigma}(A)$ denotes the non-increasing sequences of singular values of A. For future reference we also define the following dot product operator:

$$\vec{\sigma}(A) \cdot \vec{\sigma}(B) = \sum_{k=0}^{\infty} \sigma_k(A)\sigma_k(B). \qquad (24)$$

The T-suboperators in Eq. (23) are assumed to have finite Hilbert-Schmidt norm

$$\left\|T^{\lambda\lambda'}\right\|_{\mathrm{HS}}^2 := \int \frac{d^3\boldsymbol{p}}{|\boldsymbol{p}|} \frac{d^3\boldsymbol{p}'}{|\boldsymbol{p}'|} \left|T^{\lambda\lambda'}(\boldsymbol{p}, \boldsymbol{p}')\right|^2 < \infty, \qquad (25)$$

which ensures the existence of their singular value decomposition. Then, we have that

$$\left\|T^{\lambda\lambda'}\right\|_{\mathrm{HS}}^2 = \vec{\sigma}(T^{\lambda\lambda'}) \cdot \vec{\sigma}(T^{\lambda\lambda'}). \qquad (26)$$

Using the von Neumann trace inequality for Hilbert-Schmidt operators [37] we re-write the definition of em-chirality in Eq. (23) (see Appendix) as

$$\chi(T) = \sqrt{\min_{U_1 V_1} \|T^{++} - U_1 T^{--} V_1\|_{\mathrm{HS}}^2 + \min_{U_2 V_2} \|T^{-+} - U_2 T^{+-} V_2\|_{\mathrm{HS}}^2}, \qquad (27)$$

where the minimization is performed with respect to all unitary $U_{1,2}$ and $V_{1,2}$. Taking into account Sec. 2, we note that this definition can be applied to both single-frequency scattering and to scattering taking place in the whole frequency domain, in case the Hilbert-Schmidt norm of the T-operator is finite.

This measure of em-chirality is bounded by the square root of the total interaction $C_{int} = \sum_{\lambda,\lambda'} \left\|T^{\lambda\lambda'}\right\|_{\mathrm{HS}}^2$, which means that χ can be normalized to take values on the unit interval $\hat{\chi} = \frac{\chi}{\sqrt{C_{int}}} \in [0, 1]$. Objects that are transparent to all fields of particular helicity necessarily exhibit maximal em-chirality $\hat{\chi} = 1$ [9], where the hat denotes the normalized version of the definition. Further properties hold for reciprocal scatterers.

3.1 Reciprocal case

Reciprocity of a scatterer reflects the symmetry of measurement results under the exchange of the source and the detector. The reciprocity condition is defined in the plane wave basis as [38, Eq. 2.22]

$$\langle \boldsymbol{p}\lambda|T|\boldsymbol{p}'\lambda'\rangle = \langle -\boldsymbol{p}'\lambda'|T|-\boldsymbol{p}\lambda\rangle. \qquad (28)$$

---

[1]The singular value decomposition (SVD) of a compact operator is defined as

$$T^{\lambda\lambda'} = \sum_{k=1}^{\infty} \sigma_k(T^{\lambda\lambda'}) |\psi_k\rangle \langle\phi_k|$$

with unique sequence of non-increasing singular values $\sigma_k(T^{\lambda\lambda'})$ and some families of orthonormal vectors $|\psi_k\rangle$ and $|\phi_k\rangle$.

Most usual scatterers fulfill the reciprocity condition (there are exceptions, however, such as magneto-optical materials), which makes the following properties useful for numerous applications.

Consider a singular value decomposition of T^{+-} in the plane wave basis

$$T^{+-}(\boldsymbol{p}, \boldsymbol{q}) = \sum_{k=1}^{\infty} \sigma_k \, \psi_k^*(\boldsymbol{p}) \, \phi_k(\boldsymbol{q}) \tag{29}$$

for some orthonormal families of states $|\psi_k\rangle$ and $|\phi_k\rangle$. Then it follows from Eq. (28) that

$$T^{-+}(\boldsymbol{p}, \boldsymbol{q}) = T^{+-}(-\boldsymbol{q}, -\boldsymbol{p}) = \sum_{k=1}^{\infty} \sigma_k \, \psi_k^*(-\boldsymbol{q}) \, \phi_k(-\boldsymbol{p}) = \sum_{k=1}^{\infty} \sigma_k \, \xi_k^*(\boldsymbol{p}) \, \mu_k(\boldsymbol{q}) \tag{30}$$

for orthonormal families $\xi_k(\boldsymbol{p}) := \phi_k^*(-\boldsymbol{p})$ and $\mu_k(\boldsymbol{q}) := \psi_k^*(-\boldsymbol{q})$. It implies that the sequences of singular values of T^{+-} and T^{-+} are equal

$$\vec{\sigma}(T^{+-}) - \vec{\sigma}(T^{-+}) = \vec{0} \tag{31}$$

and the second term of Eq. (23) vanishes, which can be used to simplify computations.

Another property is reflected in the fact that a reciprocal object that exhibits the maximum value of normalized scalar em-chirality $\hat{\chi} = 1$ is transparent to fields of either positive or negative polarization handedness. The proof of this fact can be found in [9].

4   Complex em-chirality

Now we attempt to assign a left- or right-label to an em-chiral object. As argued in [1], no pseudoscalar property can be used for defining a proper left-right classification of general chiral objects in terms of a real number that acquires opposite signs for enantiomers and that is zero only for an *achiral* object. Most classes of objects possess the so-called chiral connectedness property, which means that chiral objects can be continuously transformed into their mirror enantiomers while staying chiral during the transformation. Then, in accordance with the intermediate value theorem, the pseudoscalar function must take a zero value at some point, which would nevertheless correspond to a *chiral* configuration. In such case one speaks of a false chiral zero.

In this subsection we show how a combination of a pseudoscalar property with a scalar chirality measure can solve the problem of false chiral zeros. We extend the normalized scalar measure of em-chirality by multiplying it with a complex exponential factor. The latter depends on the difference in interaction cross-sections of fields of opposite polarization handedness, which is a pseudoscalar property. The complex em-chirality is defined as

$$\chi_c(T) = \hat{\chi}(T) \exp(i\phi(T)), \tag{32}$$

where

$$\phi(T) := -\frac{\pi}{2} \left(\frac{\|T^{++}\|^2 + \|T^{-+}\|^2 - \|T^{+-}\|^2 - \|T^{--}\|^2}{\|T\|^2} - 1 \right) \tag{33}$$

$$= \pi \frac{\|T^{+-}\|^2 + \|T^{--}\|^2}{\|T\|^2} \in [0, \pi] \tag{34}$$

and the Hilbert-Schmidt norm is implied. The absolute value of the complex em-chirality is the normalized scalar em-chirality $|\chi_c(T)| = \hat{\chi}(T)$ and the real part $\Re(\chi_c)$ will be refered to as the handedness measure of the scatterer.

The defining property of the phase factor consists in its behavior under arbitrary mirror transformations. The T-matrix is tranformed as

$$
\begin{pmatrix} T^{++} & T^{+-} \\ T^{-+} & T^{--} \end{pmatrix} \rightarrow \begin{pmatrix} \widetilde{T}^{--} & \widetilde{T}^{-+} \\ \widetilde{T}^{+-} & \widetilde{T}^{++} \end{pmatrix}, \tag{35}
$$

where tilde indicates a reflection of a T-suboperator, which is a unitary transformation. The permutation of suboperators is due to the change of the helicity under mirror transformations.

The phase of the complex em-chirality ϕ changes under mirror transformations according to

$$
\phi(T) = \pi \frac{\|T^{+-}\|^2 + \|T^{--}\|^2}{\|T\|^2} \rightarrow \pi \frac{\|T^{-+}\|^2 + \|T^{++}\|^2}{\|T\|^2} \tag{36}
$$

$$
= \pi \frac{\|T\|^2 - \|T^{+-}\|^2 - \|T^{--}\|^2}{\|T\|^2} \tag{37}
$$

$$
= \pi - \phi(T), \tag{38}
$$

so the mirror transformation reflects the complex em-chirality with respect to the imaginary axis

$$
\hat{\chi}(T)\exp(i\phi(T)) \rightarrow \hat{\chi}(T)\exp(i(\pi - \phi(T))), \tag{39}
$$

which changes the sign of the handedness.

The complex em-chirality maps a scatterer to a semicirle of unit radius, which is divided into four distinct regions: of right-handed $\Re(\chi_c) < 0$, left-handed $\Re(\chi_c) > 0$, achiral $\chi_c = 0$, and unhanded $\Re(\chi_c) = 0$, $\chi_c \neq 0$ scatterers. This allows to distinguish between unhanded and achiral states, which constitutes the solution to the false chiral zeros problem.

Just as with the scalar em-chirality, the complex em-chirality can be defined for T-operators acting on the whole frequency domain as well as T-matrices describing monochromatic scattering. In the former case it becomes possible to define handedness for frequency-mixing scatterers. In Sec. 5 we apply complex em-chirality in monochromatic regime for a numerical illustration of chiral connectedness and the false chiral zeros problem.

One limitation of the complex em-chirality consists in the existence of unhanded states. This implies that there are pairs of enantiomers that have the same value of complex em-chirality, and therefore can not be distinguished. This problem is integral to all approaches that try to distinguish enantiomers by assigning left- and right-handed labels, which is in general not sufficient to describe the complete multidimensional nature of chirality [1]. Besides, the choice of the pseudoscalar property is rather arbitrary, so alternative pseudoscalar properties would lead to a different assignment of handedness labels. The alternative approach to analyzing chirality and distinguishing enantiomers that is free of such drawbacks will be discussed in Sec. 6. Appendix B contains further properties of complex em-chirality. In particular, that $\chi_c(T) = 1(-1)$ for objects that are invisible to light of negative(positive) helicity.

5 Illustration of chiral connectedness with complex em-chirality and solution to the false chiral zero problem

We apply the notion of complex em-chirality to study a reciprocal system of seven dielectric spheres and its continuous transformations. We start with a geometrically chiral composition of spheres with radii $r = 100$ nm and relative permittivity $\epsilon_r^s = 4$ in air ($\epsilon_r^{\text{air}} = 1$) that are centered at points $(-a, a, 0)$, $(-a, 0, 0)$, $(0, 0, 0)$, $(0, 0, a)$, $(0, a, a)$, $(a, 0, 0)$ and $(a, -a, 0)$ with $a = 500$ nm as shown in Fig. (1a). The last two spheres (the right leg of the configuration) will be continuously rotated around the y-axis by $\pi/2$ in the positive direction, such that the configuration of Fig. (1c) is achieved. The final state is the enantiomer of the initial one, which can be seen by reflecting the starting configuration with respect to the xy-plane and then rotating the resulting object about the y-axis by $\pi/2$.

We consider electromagnetic scattering properties of spheres at a fixed frequency $f = 500$ THz and calculate the T-matrix of the configuration at numerous points of the continuous transformation using a typical multiscattering algorithm [39], which is implemented in the code described in [40]. This allows to numerically compute the trajectory of the complex em-chirality χ_c for this process, the result of which is presented in Fig. (3a). The starting configuration is right-handed $\Re(\chi_c) < 0$ and the final configuration is left-handed $\Re(\chi_c) > 0$. The zero value of complex em-chirality corresponds to the arrangement of Fig. (1b), which is geometrically achiral because of its obvious mirror symmetry. As mentioned in Sec. 3, geometrically achiral objects are electromagnetically achiral, which is the reason for vanishing χ_c.

There are, however, principally different transformations that mutate the initial state Fig. (1a) into its antipode Fig. (1c) without ever reaching an achiral configuration. An example of such transformation is described on Fig. (2). This transformation is designed to avoid achiral arrangements by breaking the mirror symmetry of Fig. (1b). The corresponding trajectory of complex em-chirality on Fig. (3b) shows that at no point of this transformation the configuration becomes electromagnetically achiral. The existence of such transformations is the essence of the chiral connectedness property.

If we focus solely on the handedness part, we note that it takes a zero value at the intersection of the trajectory with the imaginary line. This point is the false chiral zero of the pseudoscalar function $\Re(\chi_c)$. Its combination with the scalar measure of em-chirality allows to unambiguously distinguish between achiral states $|\chi_c| = 0$ and states with $\Re(\chi_c) = 0$, which constitutes the solution to the false chiral zero problem.

Configurations with $|\chi_c| \neq 0$ and $\Re(\chi_c) = 0$ can be called unhanded, because the given pseudoscalar function fails to assign a handedness to them. Such configurations are chiral, so they exist in two enantiomeric versions, but they can not be distinguished using complex em-chirality. In the next section we provide the solution to the problem of the complete description of em-chirality, which will allow to distinguish *any* pair of enantiomers by classifying objects with respect to their chirality signature.
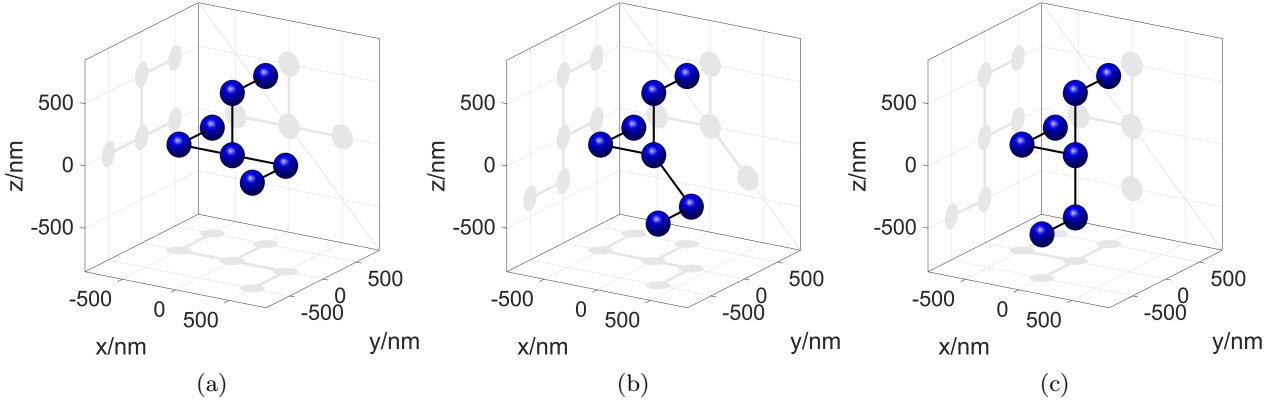
Figure 1: Continuous transformation of a chiral configuration of seven spheres (a) to its enantiomer (c) passing the achiral configuration (b): two spheres of the right leg are rotated by $\pi/2$ about the y-axis. The configuration (b) is achiral, since it is mirror symmetric with respect to the plane $z + x = 0$. The configuration (c) is the mirror antipode of the configuration (a): the mirror reflection of the initial configuration (a) with respect to the xy-plane followed by a rotation about the y-axis by $\pi/2$ results in the final configuration (c).

6 Chirality signature

The existence of chiral unhanded states $\chi_c \neq 0$, $\Re(\chi_c) = 0$ reveals the fact that complex em-chirality does not contain the full information about chiral properties of an object. The complete picture would be described by a mathematical object χ_s that, for an object T and its mirror antipode $\widetilde{T}$, fulfills the properties

$$\chi_s(T) = -\chi_s(\widetilde{T}) \tag{40}$$

$$T \text{ is em-achiral} \Rightarrow \chi_s(T) = 0 \tag{41}$$

$$\chi_s(T) = 0 \Rightarrow T \text{ is em-achiral} \tag{42}$$

Violation of Eq. (42) by the handedness part of the complex em-chirality $\Re(\chi_c)$ is the cause of unhanded states.

In our framework it is possible to define a quantity that would fulfill the properties (40) - (42). Consider the difference of the sequences of singular values

$$\vec{\chi}_1(T) = \vec{\sigma}(T^{++}) - \vec{\sigma}(T^{--}) \tag{43}$$

$$\vec{\chi}_2(T) = \vec{\sigma}(T^{+-}) - \vec{\sigma}(T^{-+}). \tag{44}$$

According to Eq. (35) and the corresponding discussion, a mirror transformation changes the sign of each element of the sequences (43)-(44):

$$\vec{\chi}_1(\widetilde{T}) = \vec{\sigma}(T^{--}) - \vec{\sigma}(T^{++}) = -\vec{\chi}_1(T) \tag{45}$$

$$\vec{\chi}_2(\widetilde{T}) = \vec{\sigma}(T^{-+}) - \vec{\sigma}(T^{+-}) = -\vec{\chi}_2(T). \tag{46}$$

Besides, the achirality condition (20)-(21) is equivalent to $\vec{\chi}_1(T) = \vec{\chi}_2(T) = \vec{0}$. This implies that the properties (40)-(42) are fulfilled by the tuple

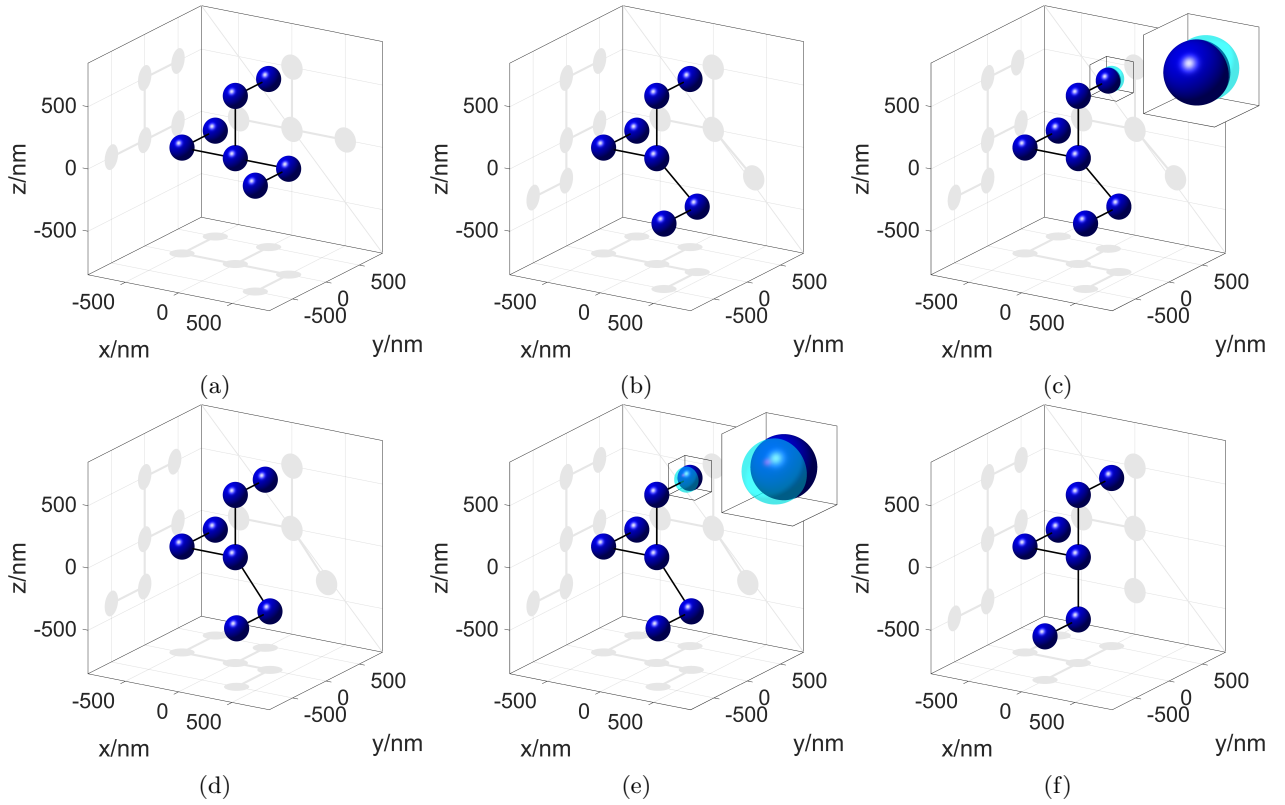$$\vec{\chi}_s(T) := (\vec{\chi}_1(T), \vec{\chi}_2(T)), \tag{47}$$

12

Figure 2: Continuous transformation of the initial configuration (a) to its enantiomer (f) avoiding any achiral configuration. The transformation is similar to the of Fig. (1), but the achiral state Fig. (1b) is avoided by introducing a perturbation in the top part of the configuration. First, the right leg is rotated about the y-axis by $9\pi/40$ (b), then the furthest top sphere is shifted by 50nm along the negative direction of the y-axis (c) – the transparent blue sphere depicts the position of the sphere before the shift (also enlarged in the top right corner). Then the right leg is rotated by extra $2\pi/40$ (d). Afterwards the shifted top sphere is brought back to its initial position (e) and finally the right leg is rotated by the remaining $9\pi/40$ to the final configuration.
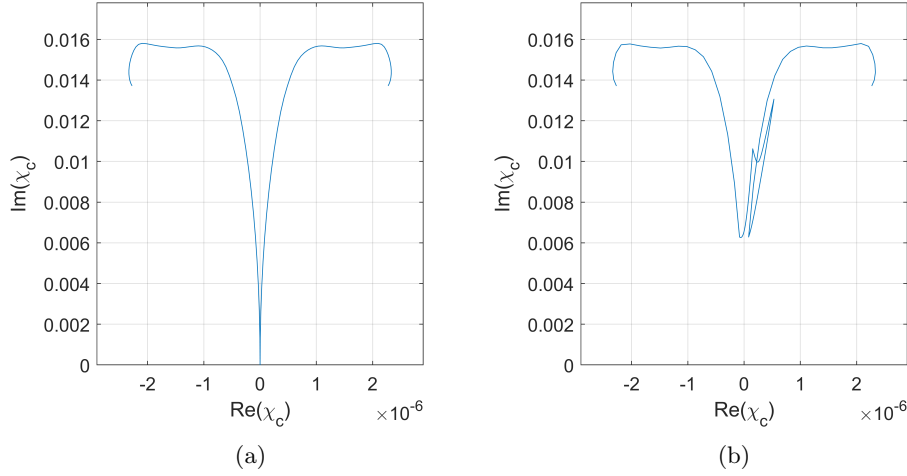
Figure 3: Trajectories of complex em-chirality for (a) the continuous transformation that passes the chiral zero (corresponds to Fig. (1)) and (b) the continuous transformation that avoids the chiral zero (corresponds to Fig. (2)). The trajectories start in the left-handed region $\Re(\chi_c) < 0$ and end in the right-handed region $\Re(\chi_c) > 0$. The absolute value of χ_c equals the scalar em-chirality and the real part is the pseudoscalar handedness measure.

which we will call the *chirality signature*.

The scalar em-chirality (Eq. (23)) can be written as a function of $\vec{\chi}_s(T)$ as

$$\chi = \sqrt{\vec{\chi}_1(T) \cdot \vec{\chi}_1(T) + \vec{\chi}_2(T) \cdot \vec{\chi}_2(T)}. \tag{48}$$

In the case of a reciprocal scatterer (31) the second part of the tuple vanishes

$$\vec{\chi}_2(T) = \vec{0}, \tag{49}$$

and the chirality signature may be identified just with the sequence $\vec{\chi}_1$

$$\vec{\chi}_s(T) := \vec{\chi}_1(T). \tag{50}$$

We provide an illustration for this definition using the reciprocal system from the previous section. The values of $\vec{\chi}_s(T_a)$, $\vec{\chi}_s(T_b)$ and $\vec{\chi}_s(T_c)$ are shown in Fig. (4), where the T-matrices correspond to the configurations described on Figs. (1a) - (1c).

As can be seen on Fig. (4), the components of the chirality signature of enantiomeric configurations have opposite signs

$$\vec{\chi}_s(T_a) = -\vec{\chi}_s(T_c) \tag{51}$$

and the chirality signature of the achiral configuration has only zero components

$$\vec{\chi}_s(T_b) = \vec{0}. \tag{52}$$

An important property of the chirality signature consists in the fact that its components converge to zero: they consist of differences of ordered singular values, which decrease as the singular value index increases. This allows to
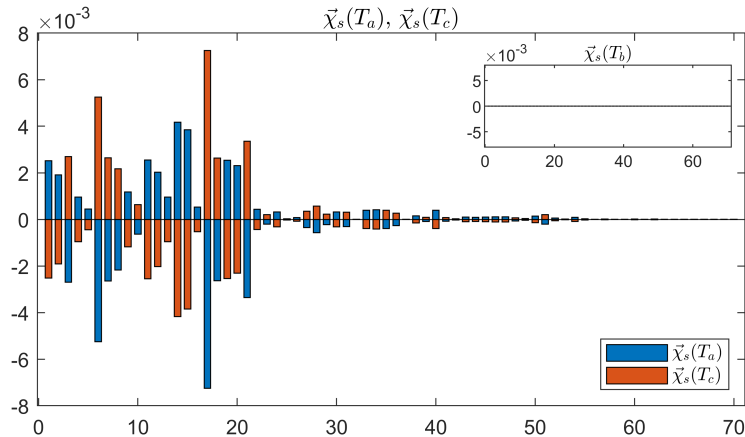
14

Figure 4: First 70 components of the chirality signature for the initial T_a, achiral T_b and final T_c configurations from Fig. (1). The mirror antipodes have components of opposite signs $\vec{\chi}_s(T_a) = -\vec{\chi}_s(T_c)$ and the achiral configuration has all components equal to zero $\vec{\chi}_s(T_b) = \vec{0}$. The square root of the sum of the squares of the components equals the scalar em-chirality $\hat{\chi} = 0.014$.

truncate the chirality signature from some point, saving the significant part that contributes to the scalar em-chirality.

Each component of $\vec{\chi}_s$ acts as an independent pseudoscalar handedness measure: it changes its sign under a mirror transformation and equals zero if the object is achiral. An individual component of $\vec{\chi}_s$ sometimes equals zero for a chiral state, producing a false chiral zero. But only when *all* the elements of $\vec{\chi}_s$ equal zero, the object is em-achiral. This provides, for the first time, the concrete quantification of the infinite-dimensional nature of chirality that Weinberg and Mislow envisioned in [1].

We note that the chirality signature method is fundamentally different from the conventional approach, where enantiomers are distinguished by a single pseudoscalar property such as optical rotation or circular dichroism. Such properties are typically very small and can be zero for chiral objects. A property such as this one was incorporated in the phase of complex em-chirality. As one can see on Fig. (3), the handedness part of complex em-chirality (the real part of χ_c) is at least 3 orders of magnitude smaller than the corresponding scalar em-chirality (the absolute value of χ_c). This implies that the contribution of the selected pseudoscalar property to the scalar em-chirality has very low significance for our system. In fact, the handedness part of the computed χ_c is smaller than the 70'th component of the chirality signature $\vec{\chi}_s$.

The chirality signature, on the other hand, provides the complete (as defined by Eqs. (40)-(42)) decomposition of scalar em-chirality into its pseudoscalar components. This, together with the fact that its norm $\vec{\chi}_s$ equals the scalar em-chirality $\hat{\chi}$, results in the access to significant pseudoscalar functions of the object. These are of the same order of magnitude as the scalar em-chirality, as seen on Fig. (4). Therefore, differentiation of enantiomers using this description is much more stable with respect to perturbations of the geometry of the object or to uncertainties in the entries of the T-matrix.

Opposite to the conventional approach, the chirality signature is able to
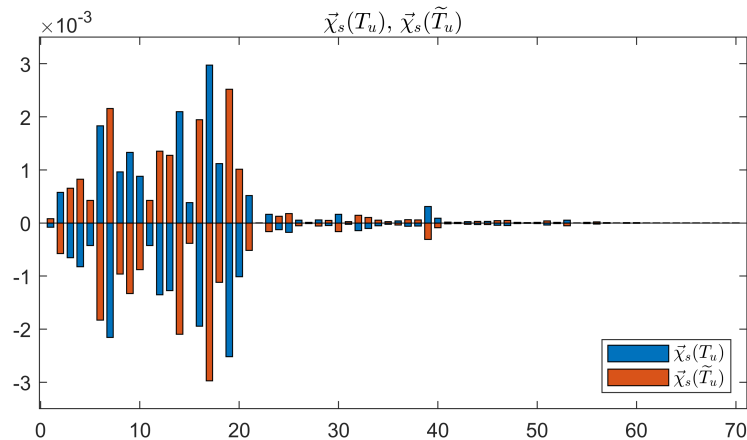
Figure 5: First 70 components of the chirality signature for the chiral unhanded configuration T_u (configuration that corresponds to the point with $\Re(\chi_c) = 0$ on Fig. (3b)) and the chirality signature of its enantiomer $\widetilde{T}_u$. Chirality signature is able to distinguish both enantiomers, while the complex em-chirality has the same value for both $\chi_c(T_u) = \chi_c(\widetilde{T}_u)$.

continuously distinguish *any* pair of enantiomers. An example of the failure of the conventional approach is the state T_u that corresponds to the chiral unhanded state $\Re(\chi_c) = 0$ on Fig. (3b). Since the configuration is chiral, there exist its geometric enantiomer $\widetilde{T}_u$. But both of them acquire the same value of complex em-chirality

$$\chi_c(T_u) = \chi_c(\widetilde{T}_u).\tag{53}$$

In this case the complex em-chirality is unable to differentiate these particular enantiomers. The chirality signature, however, provides two different pseudovectors for T_u and for $\widetilde{T}_u$, as shown on Fig. (5).

7   Conformal invariance

The conformal group constitutes the largest symmetry group of Maxwell's equations [41]. It consists of the ten-parameter Poincaré group (four space-time translations, three rotations and three Lorentz boosts) together with a dilation and four special conformal transformations. Before proving the conformal invariance of the introduced em-chirality measures (in the polychromatic regime) we first prove their Poincaré invariance. The states (16) transform unitarily under a general Poincaré tranformation Π with helicity λ unchanged [30]:

$$\Pi \,|\boldsymbol{p}\,\lambda\rangle = |\Pi\boldsymbol{p}\,\lambda\rangle \, e^{-i\alpha(\Pi,\boldsymbol{p},\lambda)}.\tag{54}$$

This means that each of the four scattering suboperators $T^{\lambda\lambda'}$ (defined on the whole frequency domain) will transform independently and without changing its singular values:

$$T^{\lambda\lambda'} = \sum_k \sigma_k \,|\psi_k\rangle \,\langle\phi_k| \rightarrow \sum_k \sigma_k \Pi \,|\psi_k\rangle \,\langle\phi_k|\,\Pi^\dagger = \sum_k \sigma_k \,|\psi_k'\rangle \,\langle\phi_k'|\tag{55}$$

16

where $|\psi'_k\rangle = \Pi |\psi_k\rangle$ and $|\phi'_k\rangle = \Pi |\phi_k\rangle$ are new families of orthonormal vectors. It the follows from Eq. (26) that the norms of suboperators are invariant under unitary transformations as well. This implies that the em-chirality (23), the complex em-chirality (32) and the chirality signature (47) are invariant under Poincaré transformations. We now show the conformal invariance.

As proven in [42], a massless irreducible representation of the Poincaré group can be extended to a representation of the conformal group by defining the generators of dilation and special conformal transformations as (we reproduce the equations from the original article without any changes)

$$D = \frac{1}{2}[P_0 P_k / P^2, J_{0k}]_+ \tag{56}$$

$$K_0 = \frac{1}{2}[P_0 / P^2, J_{0k} J_{0k} + \Lambda^2 - 1/2]_+ \tag{57}$$

$$K_i = \frac{1}{2}[P_0 / P^2, [J_{0k}, J_{ik}]_+]_+ - \frac{1}{2}[P_i / P^2, J_{0k} J_{0k} + \Lambda^2 - 1/2]_+, \tag{58}$$

where the sums over $k = 1, 2, 3$ are implied, P_μ and $J_{\mu\nu}$ are generators of the Poincaré group, Λ is the helicity operator and $[\cdot, \cdot]_+$ is the anti-commutator.

If the Poincaré group is represented unitarily, which is our case, then the extension to the conformal group representation is also unitary [42]. Since the helicity operator Λ commutes with all elements of the Poincaré group, it is evident from Eqs. (56)-(58) that it also commutes with all the conformal generators, which means that helicity is unchanged by conformal tranformations. The singular values of T-suboperators are unchanged under the unitary conformal transformations, and we conclude that all the defined measures of em-chirality are conformally invariant. Given an object and its T-matrix, the quantities $\chi(T)$, $\chi_c(T)$ and $\vec{\chi}_s(T)$ are the same for any conformally transformed version of the object. This means, in particular, that each $\vec{\chi}_s(T)$ is uniquely associated with a corresponding set of objects, where all objects in the set are related to each other by conformal transformations.

We note that this discussion combined with the group-theoretical representation of electromagnetic fields reveals that electromagnetic waves conserve their polarization handedness under conformal transformations. This conclusion, to the knowledge of authors, has not been previously expressed in the literature.

The fact that the results of our analysis are conformally symmetric is a rare circumstance. Most physical properties, such as energy, momentum and even mass (unless it's zero) are not invariant under conformal transformations. On the contrary, the introduced chirality measures are invariant under the actions of the conformal group. Such high invariance indicates a special type of description, which only contains information that is inherent to the scatterer.

8 Final remarks

In this work, and within the context of light-matter interactions, we have solved two long-standing problems related to chirality: the false chiral zeros problem related to chiral connectedness, and the general distinction of enantiomers. We have introduced the complex electromagnetic chirality, a measure that describes the handedness of an object without acquiring false chiral zeros. We have also

introduced the chirality signature of an object: an infinite-dimensional pseudovector whose components vanish simultaneously if and only if the object is electromagnetically achiral. The chirality signature provides the complete description of electromagnetic chirality, offering a continuous quantification of the multidimentional nature of chirality. Unlike conventional approaches that utilize a single pseudoscalar function, the chirality signature provides a consistent and general method for continuously distinguishing each element of any pair of enantiomers. We have proved that the scalar and complex electromagnetic chirality measures, as well as the chirality signature, are invariant under all the transformations of the conformal group. Historically, the study of invariance and symmetry concepts was often key to extending our physical understanding. The complete and conformally invariant quantification of electromagnetic chirality provided by the chirality signature distinguishes it as a particularly suitable tool for the study of chirality and its applications.

9 Acknowledgments

A Proof of the new formula for scalar em-chirality

First we show that, for any two Hilbert-Schmidt operators A and B, it holds that

$$\min_{U,V} \|A - UBV^\dagger\|_{\mathrm{HS}}^2 = |\vec{\sigma}(A) - \vec{\sigma}(B)|^2, \tag{59}$$

where the minimization takes place over unitary operators U and V, $\vec{\sigma}(A)$ and $\vec{\sigma}(B)$ are non-increasing sequences of singular values, $|\vec{\sigma}(A) - \vec{\sigma}(B)|^2 = (\vec{\sigma}(A) - \vec{\sigma}(B)) \cdot (\vec{\sigma}(A) - \vec{\sigma}(B))$, and the $\cdot$ operation is defined in Eq. (24).

Using the Hilbert-Schmidt scalar product we re-write the left hand side as

$$\min_{U,V} \|A - UBV^\dagger\|_{\mathrm{HS}}^2 = \tag{60}$$

$$= \min_{U,V} \langle A - UBV^\dagger, \ A - UBV^\dagger \rangle \tag{61}$$

$$= \min_{U,V} \left\{ \langle A, A \rangle + \langle UBV^\dagger, UBV^\dagger \rangle - \langle A, UBV^\dagger \rangle - \langle UBV^\dagger, A \rangle \right\} \tag{62}$$

$$= \|A\|_{\mathrm{HS}}^2 + \|UBV^\dagger\|_{\mathrm{HS}}^2 - \max_{U,V} \left\{ \langle UBV^\dagger, A \rangle + \langle A, UBV^\dagger \rangle \right\} \tag{63}$$

$$= \|A\|_{\mathrm{HS}}^2 + \|B\|_{\mathrm{HS}}^2 - 2 \max_{U,V} \left\{ \mathrm{Re} \langle A, UBV^\dagger \rangle \right\}. \tag{64}$$

and the problem reduces to maximizing $\mathrm{Re} \langle A, UBV^\dagger \rangle$. The von Neumann trace inequality for Hilbert-Schmidt operators states [37] that any two Hilbert-Schmidt operators X, Y fulfill the condition

$$\mathrm{Re} \langle X, Y \rangle \leq \sum_{k=1}^{\infty} \sigma_k(X)\sigma_k(Y) \tag{65}$$

18

with equality holding if and only if X and Y share singular vectors. It is always possible to find such unitary U and V that transform the singular vectors of B onto those of A by the following construction. Consider singular value decompositions of A and B

$$A = U_a \Sigma_a V_a^\dagger \tag{66}$$

$$B = U_b \Sigma_b V_b^\dagger. \tag{67}$$

Then for

$$U \coloneqq U_a U_b^\dagger \tag{68}$$

$$V \coloneqq V_a V_b^\dagger \tag{69}$$

one gets

$$UBV^\dagger = U_a U_b^\dagger U_b \Sigma_b V_b^\dagger (V_a V_b^\dagger)^\dagger = U_a \Sigma_b V_a^\dagger, \tag{70}$$

which according to the von Neumann trace inequality realizes the maximal value

$$\max_{U,V} \left\{ \mathrm{Re} \langle A, UBV \rangle \right\} = \sum_{k=1}^{\infty} \sigma_k(A)\sigma_k(B) = \vec{\sigma}(A) \cdot \vec{\sigma}(B). \tag{71}$$

Now, using $\|A\|_{\mathrm{HS}}^2 = \vec{\sigma}(A) \cdot \vec{\sigma}(A) \coloneqq \vec{\sigma}^2(A)$, where a shorthand notation is introduced after the $\coloneqq$ symbol, and, similarly $\|B\|_{\mathrm{HS}}^2 = \vec{\sigma}^2(B)$, we finally write Eq. (64) as

$$\min_{U,V} \|A - UBV^\dagger\|_{\mathrm{HS}}^2 = \vec{\sigma}^2(A) + \vec{\sigma}^2(B) - 2\,\vec{\sigma}(A) \cdot \vec{\sigma}(B) \tag{72}$$

$$= |\vec{\sigma}(A) - \vec{\sigma}(B)|^2. \tag{73}$$

Application of this formula to the definition of the scalar em-chirality (23) results in

$$\chi^2(T) = |\vec{\sigma}(T^{++}) - \vec{\sigma}(T^{--})|^2 + |\vec{\sigma}(T^{+-}) - \vec{\sigma}(T^{-+})|^2 \tag{74}$$

$$= \min_{U_1 V_1} \|T^{++} - U_1 T^{--} V_1\|_{\mathrm{HS}}^2 + \min_{U_2 V_2} \|T^{-+} - U_2 T^{+-} V_2\|_{\mathrm{HS}}^2, \tag{75}$$

which provides a new perspective on scalar em-chirality as the solution to a minimization problem. One can recognize a close resemblance to the well-known orthogonal Procrustes problem [43], but formulated for Hilbert-Schmidt operators acting on the space of solutions to Maxwell's equations. The definition of em-chirality in Eq. (75) lends itself to straightforward formulations of T-matrix-based scalar measures of geometrical chirality. It suffices to restrict the U_i/V_i to compositions of rotations and translations. Such an approach was studied in [44].

B Further properties of complex em-chirality

Consider a scatterer that is transparent to fields of positive helicity. Then, as was mentioned in Sec. 3, it exhibits the maximal scalar em-chirality $\hat{\chi} = 1 = |\chi_c|$. The phase (34) can be found using

$$\|T^{++}\|^2 = \|T^{-+}\|^2 = 0, \tag{76}$$

which implies $\phi = \pi$ and it follows that the object is maximally right-handed

$$\chi_c(T) = -1. \tag{77}$$

In the case of transparency to fields of negative helicity we similarly have $\chi = 1$ together with

$$\|T^{--}\|^2 = \|T^{+-}\|^2 = 0, \tag{78}$$

so $\phi = 0$ and the object is maximally left-handed

$$\chi_c(T) = 1. \tag{79}$$

The converse is true for reciprocal objects. Assuming maximal scalar em-chirality $\hat{\chi} = 1 = |\chi_c|$ and the condition (31), we get for the normalized version of the definition (23)

$$1 = \frac{(\vec{\sigma}(T^{++}) - \vec{\sigma}(T^{--}))^2}{\vec{\sigma}(T^{++})^2 + \vec{\sigma}(T^{+-})^2 + \vec{\sigma}(T^{-+})^2 + \vec{\sigma}(T^{--})^2} \tag{80}$$

and therefore

$$\vec{\sigma}(T^{+-})^2 + \vec{\sigma}(T^{-+})^2 = -2\,\vec{\sigma}(T^{++}) \cdot \vec{\sigma}(T^{--}), \tag{81}$$

where the dot product denotes $\sum_{k=1}^{\infty} \sigma_k(T^{++})\sigma_k(T^{--})$. Since singular values are non-negative, there exist only two possibilities for this condition to be fulfilled: either

$$\vec{\sigma}(T^{+-}) = \vec{0}, \quad \vec{\sigma}(T^{-+}) = \vec{0}, \quad \vec{\sigma}(T^{++}) = \vec{0} \tag{82}$$

or

$$\vec{\sigma}(T^{+-}) = \vec{0}, \quad \vec{\sigma}(T^{-+}) = \vec{0}, \quad \vec{\sigma}(T^{--}) = \vec{0}. \tag{83}$$

If all singular values of an operator are zero, then the operator itself is zero, hence both cases signify invisibility to fields of positive and negative helicity respectively. The first case (82) implies $\phi = \pi$ and consequently the object is maximally right-handed $\chi_c = -1$, the second case (83) results in $\phi = 0$ and the maximal left-handedness $\chi_c = 1$ follows.

References

[1] Noham Weinberg and Kurt Mislow. On chirality measures and chirality properties. *Canadian Journal of Chemistry*, 78(1):41–45, 2000.

[2] Paul Mezey. Rules on chiral and achiral molecular transformations. *Journal of Mathematical Chemistry*, 17:185–202, 06 1995.

[3] Noham Weinberg and Kurt Mislow. On chiral pathways in E(n): A dimensional analysis. *Theoretica Chimica Acta*, 95(3):63–65, 1997.

[4] Patrick W. Fowler. Quantification of chirality: Attempting the impossible. *Symmetry: Culture and Science*, 16(4):321–334, 2005.

[5] P.C. Waterman. Matrix formulation of electromagnetic scattering. *Proceedings of the IEEE*, 53(8):805–812, 1965.

[6] Michael I. Mishchenko, Larry D. Travis, and Daniel W. Mackowski. T-matrix computations of light scattering by nonspherical particles: A review. *Journal of Quantitative Spectroscopy and Radiative Transfer*, 55(5):535–575, 1996.

[7] T-matrix codes. `https://scattport.org/index.php/programs-menu/t-matrix-codes-menu`. Accessed: 2021-10-28.

[8] Ivan Fernandez-Corbaton, Dominik Beutel, Carsten Rockstuhl, Ansgar Pausch, and Wim Klopper. Computation of electromagnetic properties of molecular ensembles. *ChemPhysChem*, 21(9):878–887, 2020.

[9] Ivan Fernandez-Corbaton, Martin Fruhnert, and Carsten Rockstuhl. Objects of maximum electromagnetic chirality. *Phys. Rev. X*, 6:031013, Jul 2016.

[10] Maxim V. Gorkunov, Alexander A. Antonov, and Yuri S. Kivshar. Metasurfaces with maximum chirality empowered by bound states in the continuum. *Phys. Rev. Lett.*, 125:093903, Aug 2020.

[11] Tilo Arens, Roland Griesmaier, and Marvin Knöller. Maximizing the electromagnetic chirality of thin dielectric tubes. *SIAM Journal on Applied Mathematics*, 81(5):1979–2006, 2021.

[12] Xavier Garcia-Santiago, Martin Hammerschmidt, Sven Burger, Johannes Sachs, Hyunah Kwon, Peer Fisher, Marvin Knoeller, Tilo Arens, Frank Hettlich, Roland Griesmaier, Ivan Fernandez-Corbaton, and Carsten Rockstuhl. Towards maximal electromagnetically chiral scatterers at optical frequencies. *In preparation*, 2021.

[13] Tilo Arens, Felix Hagemann, Frank Hettlich, and Andreas Kirsch. The definition and measurement of electromagnetic chirality. *Mathematical Methods in the Applied Sciences*, 41(2):559–572, 2018.

[14] Ioannis G. Stratis. Chirality notions and electromagnetic scattering: a mini review. *Complex Variables and Elliptic Equations*, 0(0):1–33, 2021.

[15] Muamer Kadic, Graeme W. Milton, Martin van Hecke, and Martin Wegener. 3D metamaterials. *Nature Reviews Physics*, 1(3):198–210, Mar 2019.

[16] Ivan Fernandez-Corbaton, Xavier Vidal, Nora Tischler, and Gabriel Molina-Terriza. Necessary symmetry conditions for the rotation of light. *J. Chem. Phys*, 138(21), 2013.

[17] Antoine Canaguier-Durand, James A. Hutchison, Cyriaque Genet, and Thomas W. Ebbesen. Mechanical separation of chiral dipoles by chiral light. *New J. Phys.*, 15(12):123037, 2013.

[18] Matt M. Coles, Mathew D. Williams, Kamel Saadi, David S. Bradshaw, and David L. Andrews. Chiral nanoemitter array: A launchpad for optical vortices. *Laser & Photonics Reviews*, 7(6):1088–1092, 2013.

[19] Konstantin Y. Bliokh, Yuri S. Kivshar, and Franco Nori. Magnetoelectric effects in local light-matter interactions. *Phys. Rev. Lett.*, 113(3):033601, 2014.

[20] Robert P. Cameron, Stephen M. Barnett, and Alison M. Yao. Discriminatory optical force for chiral molecules. *New J. Phys.*, 16(1):013020, 2014.

[21] Efi Efrati and William T. M. Irvine. Orientation-dependent handedness and chiral design. *Phys. Rev. X*, 4(1):011003, 2014.

[22] Manuel Nieto-Vesperinas. Optical theorem for the conservation of electromagnetic helicity: Significance for molecular energy transfer and enantiomeric discrimination by circular dichroism. *Phys. Rev. A*, 92(2):023813, 2015.

[23] Lisa V. Poulikakos, Philipp Gutsche, Kevin M. McPeak, Sven Burger, Jens Niegemann, Christian Hafner, and David J. Norris. Optical chirality flux as a useful far-field probe of chiral near fields. *ACS Photonics*, 3(9):1619–1625, 2016.

[24] David L. Andrews. Symmetries, conserved properties, tensor representations, and irreducible forms in molecular quantum electrodynamics. *Symmetry*, 10(7):298, 2018.

[25] Gutsche Philipp and Nieto-Vesperinas Manuel. Optical Chirality of Time-Harmonic Wavefields for Classification of Scatterers. *Scientific Reports*, 8(1):9416, 2018.

[26] Frances Crimin, Neel Mackinnon, Jörg B Götte, and Stephen M Barnett. On the conservation of helicity in a chiral medium. *J. Opt.*, 21(9):094003, aug 2019.

[27] Lisa V. Poulikakos, Jennifer A. Dionne, and Aitzol García-Etxarri. Optical helicity and optical chirality in free space and in the presence of matter. *Symmetry*, 11(9):1113, Sep 2019.

[28] Mina Hanifeh, Mohammad Albooyeh, and Filippo Capolino. Optimally chiral light: Upper bound of helicity density of structured light for chirality detection of matter at nanoscale. *ACS Photonics*, 7(10):2682–2691, Oct 2020.

[29] Ivan Fernandez-Corbaton. Total helicity of electromagnetic fields and matter. *Phys. Rev. B*, 103:054406, Feb 2021.

[30] Wu-Ki Tung. *Group theory in physics*. World Scientific, 1985.

[31] John David Jackson. *Classical electrodynamics*. Wiley, New York, NY, 3rd ed. edition, 1999.

[32] Harry E. Moses. Photon wave functions and the exact electromagnetic matrix elements for hydrogenic atoms. *Phys. Rev. A*, 8:1710–1721, Oct 1973.

[33] Bo Peterson and Staffan Ström. T-matrix for electromagnetic scattering from an arbitrary number of scatterers and representations of E(3). *Physical review D*, 8(10):3661, 1973.

[34] Leonard Gross. Norm invariance of mass-zero equations under the conformal group. *Journal of Mathematical Physics*, 5(5):687–695, 1964.

[35] J. Haantjes. Die Gleichberechtigung gleichförmig beschleunigter Beobachter für die elektromagnetischen Erscheinungen. *Nederl. Akademie van Wetenschappen, Proc. Section of Sciences*, 43:1288–1299, 1940.

[36] C. Codirla and H. Osborn. Conformal invariance and electrodynamics: Applications and general formalism. *Annals of Physics*, 260:91–116, 1997.

[37] Marcus Carlsson. von Neumann's trace inequality for Hilbert–Schmidt operators. *Expositiones Mathematicae*, 39(1):149–157, 2021.

[38] Riccardo Sapienza. *Photonic nano materials: anisotropic transport and optical Bloch oscillations*. PhD thesis, Université Pierre et Marie Curie - Paris VI, 2005.

[39] Michael I. Mishchenko. Comprehensive thematic T-matrix reference database: a 2017-2019 update. *Journal of Quantitative Spectroscopy and Radiative Transfer*, 242:106692, 2020.

[40] Dominik Beutel, Achim Groner, Carsten Rockstuhl, and Ivan Fernandez-Corbaton. Efficient simulation of biperiodic, layered structures based on the T-matrix method. *JOSA B*, 38(6):1782–1791, 2021.

[41] Robert Gilmore. *Lie groups, Lie algebras, and some of their applications*. Courier Corporation, 2012.

[42] V. I. Fushchich and A. G. Nikitin. Conformal invariance of relativistic equations for arbitrary spin particles. *Letters in Mathematical Physics*, 2(6):471–475, Nov 1978.

[43] John C. Gower and Garmt B. Dijksterhuis. *Procrustes problems*. Oxford University Press on Demand, 2004.

[44] Philipp Gutsche, Xavier Garcia-Santiago, Philipp-Immanuel Schneider, Kevin M. McPeak, Manuel Nieto-Vesperinas, and Sven Burger. Role of geometric shape in chiral optics. *Symmetry*, 12(1), 2020.